Optimization Strategy to Solve Transmission Interruption Caused by Satellite-Ground Link Switching

JIRUI ZHANG [1,2], **SHIBING ZHU** [3], **HEFENG BAI** [2], **AND CHANGQING LI** [3]

[1]Graduate School, Space Engineering University, Beijing 101416, China
[2]Beijing Institute of Tracking and Telecommunications Technology, Beijing 100094, China
[3]School of Space Information, Space Engineering University, Beijing 101416, China

Corresponding author: Jirui Zhang (09211210@bjtu.edu.cn)

ABSTRACT Low earth orbit (LEO) satellite systems, an important part of the next generation of global communication systems, have the advantages of low transmission delay, low satellite cost and low launch cost. The construction of an LEO satellite network with global coverage has become the direction of future space network transmission development. Although extensive research has been conducted on the routing of LEO satellite networks, most papers focus on only space segment routing, with little attention paid to the route between the satellite and ground station. This paper introduces the transmission scenario of ground station switching with connected satellites and analyzes the problem of data packet loss caused by ground station and satellite communication link switching. Two optimization strategies based on static routing and dynamic routing are proposed as solutions to the problem of data packet loss, with software-simulated test results showing that both approaches can effectively avoid packet loss.

INDEX TERMS Routing, ground station, satellite, switching.

I. INTRODUCTION

With the continuous development and advancement of aerospace science and technology, space has gradually become the focus of global attention and competition. The number of spacecraft in space has increased rapidly due to the acceleration of space development in various countries. Space networks have obvious advantages over traditional terrestrial networks in terms of invulnerability and coverage and the ability to truly realize global interconnection. Compared with geostationary earth orbit or medium earth orbit satellite systems, low earth orbit (LEO) satellite systems have the advantages of low transmission delay, low satellite cost and low launch cost. Therefore, construction of a LEO satellite network with global coverage is an important development trend for the next generation of global communication systems.

The integration of navigation, communication and detection is another future development trend of LEO satellites [1], [2]. In addition to basic communication capabilities, LEO satellite networks can provide diverse and customized

The associate editor coordinating the review of this manuscript and approving it for publication was Thanh Ngoc Dinh.

services, such as navigation, positioning, remote sensing and mapping. Due to the advantages of low delay and short transmission distance, LEO satellite networks can greatly improve the efficiency of information acquisition and transmission. LEO satellite network routing technology involves mainly satellite networks constructed by laser and microwave links between the satellites and the ground, including space segment routing and satellite-ground routing.

Current research on space segment routing of LEO satellite networks can be divided into static routing and dynamic routing. Static routing is represented by the snap shot sequence routing algorithm proposed by Werner [3]. The core of this algorithm is to divide continuous time into multiple time slices, with the node connection situation in each time slice remaining relatively stable, such that the dynamically changing connection relationship can be transformed into multiple topologically stable static connection diagrams. This algorithm was considerably improved and supplemented by later scholars [4]– [6]. Dynamic routing is represented by the datagram routing algorithm (DRA) proposed by Ekici *et al.* [7]. The DRA uses the virtual node's topology control strategy to shield the impact of high-speed

satellite movement, and each satellite independently calculates the next hop node. Other examples of dynamic routing algorithms include the darting algorithm [8], Bellman-Ford algorithm [9], and location-assisted on-demand routing algorithm [10]. In dynamic routing, the satellite can adjust the routing strategy as the network changes, which requires the satellite to have on-board processing capabilities.

In addition to space segment routing, satellite-ground routing has attracted the attention of researchers. Wu proposed a method that can maintain communication under satellite-ground link switching [11]. Yang proposed to solve the access service resource conflict caused by satellite handover [12]. Maria proposed the signal strength related to elevation angle as another satellite switching standard [13], [14]. Younes analyzed the coverage time of users in LEO satellite networks and deduced the expected inter-satellite links (ISL) handover lower limit [15]. Hu analyzed the dynamic satellite handover prediction problem to solve the problem of multiple link state changing with the user's mobile satellite [16]. Wu summarized ISL handoff standards and proposed a graph-based ISL handoff prediction framework to flexibly merge all existing satellite handoff standards [17].

Although scholars have done substantial work on the satellite-ground routing of LEO satellite networks, they have focused on how to achieve efficient and stable connectivity with the ground station when switching connected satellites [18]–[20]. Little research has been conducted on the failure of the "last hop" routing in space segment routing, which makes satellite-ground routing invalid, especially the problem of data transmission interruption when the ground station and the connected satellite switch. In this paper, we call this problem satellite-ground link switching interruption (SGLSI), which is defined as ''the data packet loss caused by failure of the original transmission path resulting from the switching of the satellite connected with the ground station.''

To overcome the packet loss caused by SGLSI, we analyze the causes of SGLSI in detail and propose two optimization strategies for satellite-ground links based on spatial static routing and dynamic routing. Considering the load change of the space network, we introduce queuing delay to verify whether the two optimization strategies are suitable for complex network scenarios and perform simulation verification. The experimental results show that the two optimization strategies can be used in different scenarios to effectively avoid data loss caused by SGLSI.

The remainder of the paper is structured as follows. In section II, we describe the problem of SGLSI and discuss when SGLSI will occur. In section III, we establish the satellite motion model and the satellite-ground transmission link model, which lead to interruption of satellite-ground link transmission, and analyze the time of link switching. In section IV, we propose two optimization strategies to solve the packet loss problem caused by the switching between the connected satellite and ground station. The feasibility of the strategies is verified via software simulation in section V, with
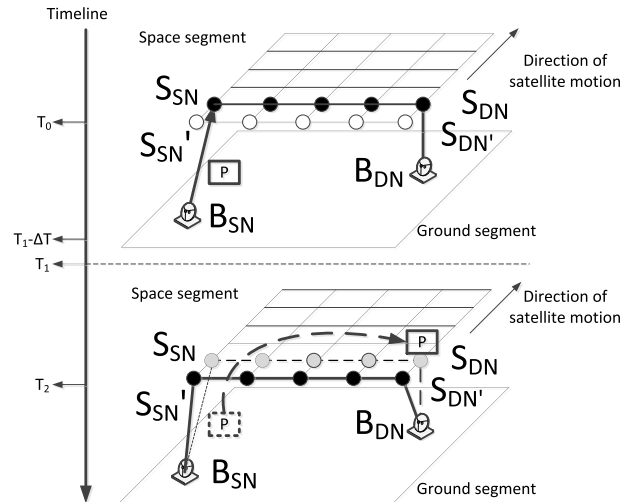

FIGURE 1. Data packet loss caused by SGLSI.

the results showing that both strategies can effectively avoid packet loss. Two optimization strategies are summarized in section VI, and directions for future work are discussed.

II. PROBLEM STATEMENT
Scholars have studied packet loss caused by satellite link switching. Raines discovered and discussed the instantaneous routing loops in satellite networks due to topology updates [20]. Partridge discussed the use of time to live domain in the Internet protocol datagram, which refers to instantaneous and long-term routing loops [21]. Kim analyzed the routing loop caused by path switching during call migration in the link-oriented LEO satellite network [22]. Tang analyzed the transmission failure caused by predictable link switching and unpredictable link switching and proposed optimization methods based on snapshot prediction and route multicast [23], [24]. In addition, some solutions have been proposed to avoid packet loss caused by link switching in the ground network [25], [26]. Nevertheless, by exclusively analyzing the packet loss caused by link switching in the space or ground segment, scholars have ignored the path failure caused by link switching between space and the ground.

For convenience of description, all ground facilities, including satellite ground stations, satellite communication vehicles and handheld terminals, are collectively referred to as ground stations in this paper. Data transmission before and after satellite switching should be considered in the process of interaction with the ground station [27]–[29].

As shown in Fig. 1, at time T_0, destination node ground station B_{DN} is in communication with destination node satellite S_{DN}, and the received data comes from S_{DN}. Since the transmission of data is random, it is assumed that at time $(T_1 - \Delta T)$ (ΔT is an infinitely small time slice), B_{SN} starts to transmit packet P, and the destination node is B_{DN}. At time T_0, S_{DN} receives data packet P, but at this time, the connected satellite of B_{DN} has changed from S_{DN} to S'_{DN}; therefore, data packet P cannot reach B_{DN} along the originally planned path. As a result, SGLSI occurs.
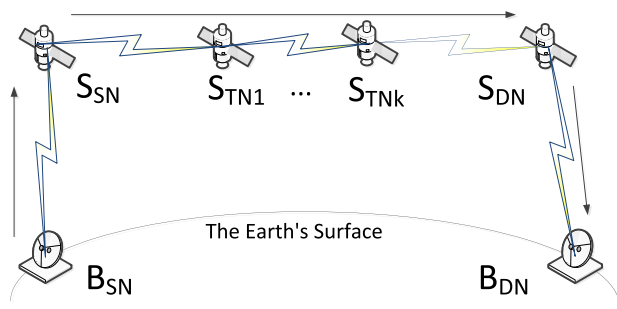
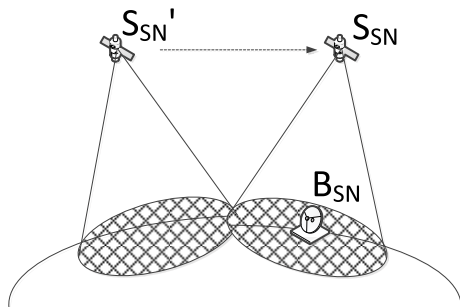**FIGURE 2.** Cross region transmission between source node ground station and destination node ground station.

FIGURE 3. Ground station of source node switching connected satellites.

FIGURE 4. Timing of connection between the ground station of the source node and the source node satellite.

FIGURE 5. Ground station of destination node switching connected satellites.

FIGURE 6. Timing of the connection between the ground station of the destination node and the destination node satellite.

Fig. 2 shows a complete transport path containing the source node ground station, destination node ground station and satellites. The figure can be used to analyze the timing of SGLSI. The transmission process between ground stations can be described as follows: when source node ground station B_{SN} sends data to destination node ground station B_{DN}, B_{SN} uploads the data to the source node satellite S_{SN} connected to it. After passing through k relay node satellite transmission, the data reach the destination node satellite S_{DN} connected to B_{DN}. S_{DN} transmits the data to B_{DN} to complete the information transmission of the whole link.

For the transmission between source node ground station and source node satellite, at least one satellite can be connected at all times during the constellation design process [30]. Therefore, when the satellite S_{SN} connected to B_{SN} is switched, it is only necessary to update S_{SN} to S'_{DN}, and the ground-to-satellite link is always connected, as shown in Fig. 3.

Although coverage areas overlap, there is always an absolute switching opportunity. Therefore, it may be assumed that the transit period of the LEO satellite network relative to the ground station is t, that is, the communication time between a satellite and a ground station. As shown in Fig. 4, the ground station of source node B_{SN} transmits data at time T_0, at which time B_{SN} is connected to S_{DN1}. At time T_1, the satellite connected to B_{SN} is switched from S_{SN1} to S_{SN2}. Since B_{SN} can accurately acquire the switch timing, data transmission is not affected; therefore, SGLSI will not occur in the transmission between the source node ground station and the source node satellite.
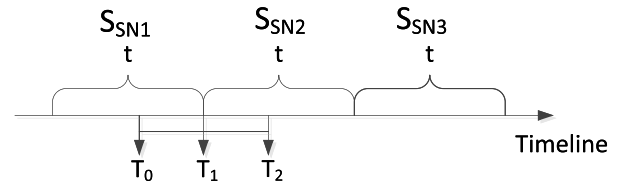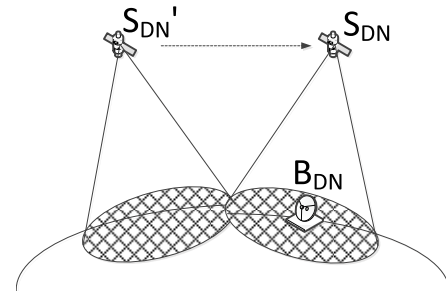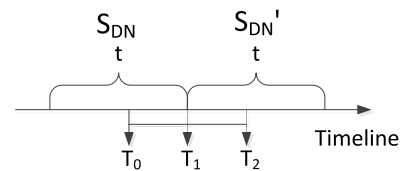
For the transmission between the destination node ground station and the destination node satellite, the destination node ground station B_{DN} must be connected to a satellite. Therefore, when the connected satellite is switched, the transmission from the ground station to the satellite will not be affected. At this time, it is necessary only to update the source node satellite S_{DN} to S'_{DN}, as shown in Fig. 5.

Now, we turn to the receiving situation of the destination node ground station. Because of the unpredictability of information transmission, it is challenging to predict when the information will reach the ground station of the destination node. As shown in Fig. 6, at time T_1, due to the transit of the original destination node satellite, the destination node satellite connected to the ground station of destination node B_{DN} is switched. At time $(T_1 - t)$, B_{DN} is connected to destination node satellite S_{DN}, and at time $(T_1 + t)$, B_{DN} remains connected to the new destination node satellite S'_{DN}. In terms of the source node, when there is a source node ground station, we usually design an overlapping portion of the coverage area for data transmitted by the ground station; consequently, the ground station can decide which satellite to choose at the time of transmission.

Therefore, SGLSI occurs only when the destination node satellite and destination node ground station transmit.

TABLE 1. Definition of the symbols.

Symbol	DEFINITION
B_{SN}	source node ground station
B_{DN}	destination node ground station
S_{SN}	source node satellite
S_{DN}	destination node satellite
S_{TN}	relay node satellite
LMS	lateral movement of the satellite
VMS	vertical movement of the satellite
R	moving radius of satellite
R_{earth}	earth radius
h	satellite's orbit height
F	centripetal force on satellite
v	linear velocity of satellite
ω	angular velocity of satellite
G	gravitational constant
M	earth weight
V	number of satellites in a single orbital plane
N	number of track surfaces
i	orbital inclination
F	phase factor
t_s	satellite time interval
t_E	orbital surface time interval
t_α	longitude arrival time (LOAT)
t_β	latitude arrival time (LAAT)
P	all data to be transferred
p_i	data packet
α	longitude of ground station
β	latitude of ground station
α_s	longitude of satellite
β_s	latitude of satellite
t_m	satellite-ground link maintenance cycle
t_{mB}	time when B_{DN} and S_{DNm} start connection
t_{mE}	time when B_{DN} and S_{DNm} end connection
t_{trans}	propagation delay
t_{data}	transmission delay
P_{trans}	amount of data packets transmitted in the B_{DN}
P_{keep}	amount of data packets that are reserved but not transmitted at the S_{DNm}

III. MODELING AND ANALYSIS

Table 1 introduces the notation that will be used throughout this paper.

Yan analyzed the Iridium system and noted that the typical single-link transmission delay of an LEO constellation is generally 10-20 ms [31]. When the network is congested, the network link queuing delay can be as high as 500 ms. Considering that future LEO satellite constellations will have a global connected network framework, the number of nodes in the network will be larger than that in the Iridium system. Considering the large scale of the satellite network designed

in the future, the switching between the satellite and the ground station will be more frequent. This section will design motion model, constellation model and satellite-ground link switching model for the LEO satellite network based on the global interconnection, and analyze the switching types of the satellite-ground links.

A. MOTION MODEL OF LEO SATELLITE

The motion of an LEO satellite can be regarded as a uniform circular motion centered on the earth's spherical center [32]. Its radius R can be derived from (1):

$$R = R_{earth} + h \tag{1}$$

where R_{earth} refers to the earth's radius and h stands for the satellite's orbit height.

The centripetal force F required for the satellite to circle the earth is provided by gravity, which is derived from the following (2) [33].

$$F = m \cdot \frac{v^2}{R} = G \cdot \frac{Mm}{R^2} \tag{2}$$

The velocity v of the circling can be derived from (3).

$$v = \omega \cdot R \tag{3}$$

When the orbit height h is fixed, the angular velocity ω of the satellite can be derived from (4):

$$\omega = \sqrt{\frac{GM}{R^3}} \tag{4}$$

where $G = 6.67 \times 10^{-11} \text{N} \cdot \text{m}^2/kg^2$ and $M = 5.965 \times 10^{24} kg$.

B. CONSTELLATION MODEL OF LEO SATELLITE NETWORK

By considering the influence that the speed of the satellite's lateral and vertical movement has on the ground station, we can predict the orbit plane of the satellite connected to the ground station [34]. Since the earth is spherical, both the earth's rotation and the satellite's periodic motion are circular motions. Therefore, it is easier and more unified to describe the motion in terms of angular rather than linear velocity. We assume for the moment some important parameters of the satellite constellation: $V \times N/N/F : h : i$. V is the number of satellites in a single orbital plane, N represents the number of orbital planes, h is the orbital height, i is the orbital inclination, F is the phase factor, which is used to represent the phase offset angle between adjacent satellites in different orbital planes, and (5) should be satisfied.

$$F \in [0, N - 1], \quad F \in Z \tag{5}$$

C. SATELLITE-GROUND LINK SWITCHING MODEL

The period of an LEO satellite network is usually approximately 2 hours because of the low orbit height and high speed [35]. In a constellation network designed for global coverage, the first condition is to ensure that every place on the ground is covered by a corresponding satellite [36]. To ensure complete satellite coverage on the ground, multiple
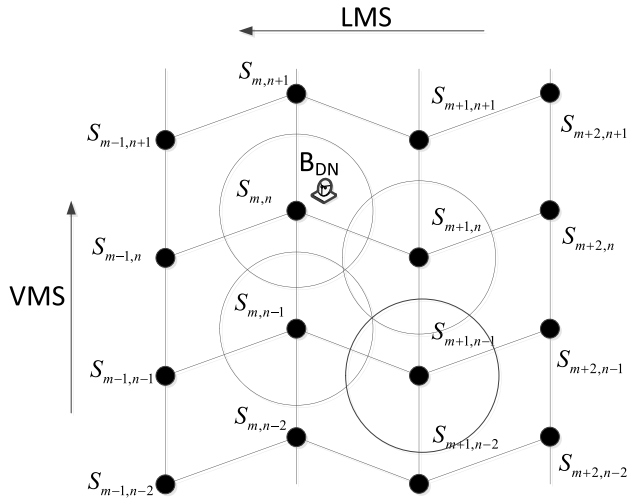
FIGURE 7. After the mobility of the shield earth station, the satellite connectivity is determined by LMS and VMS.

satellites will be designed to have overlapping coverage [37]. Therefore, which satellite is connected to the ground station is a key question.

1) KEY FACTORS AFFECTING SATELLITE-GROUND LINK CONNECTIVITY

Researchers often assume that a ground station is connected to the closest satellite [38]. The change in the connection between the ground station and the satellite is due to two factors, namely, the motion of the direct orbit of the satellite and the rotation of the earth [39].

To facilitate analysis of the switching law between the satellites and the ground station, this paper distinguishes the vertical movement of the satellite (VMS) and lateral movement of the satellite (LMS).

VMS, which refers to the celestial movement of the satellite with the earth as its circling center, is used to reflect the motion of the satellite in its own orbit.

LMS refers to the relative displacement between the satellite and the ground caused by the rotation of the earth, in which the satellite moves in the opposite direction of the earth's rotation. Due to the influence of the earth's rotation, the ground station will move to the east relative to the satellite network [40], [41]. Accordingly, considering the mobility of the shielded ground station and assuming that it is stationary, the satellite network moves westward, and the LMS parameter is introduced.

The connectivity between the ground station and the satellite is affected by LMS and VMS simultaneously.

As shown in Fig. 7, at time T_0, the satellite node connected to B_{DN} is $S_{m,n}$. Since LMS is to the left and VMS is upward, the satellite connected to B_{DN} in the next time period should be on the lower right side of the figure. Consequently, when the connectivity node of the B_{DN} is switched from $S_{m,n}$ to $S_{m',n'}$, (6) must be satisfied.

$$n' \leq n, \quad m' \geq m \qquad (6)$$
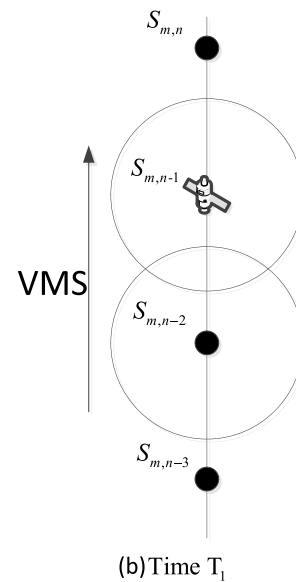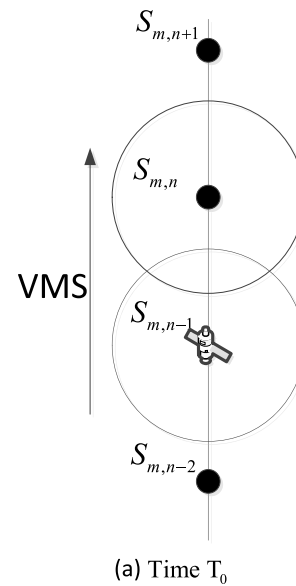

(a) Time T_0

(b) Time T_1

FIGURE 8. Analysis of satellite motion under VMS by shielding LMS.

Therefore, the next satellite node connected to B_{DN} after $S_{m,n}$ must be one of $S_{m,n-1}$, $S_{m+1,n-1}$, or $S_{m+1,n}$.

To quantitatively analyze the satellites connected with B_{DN} at the next moment, we separately analyze two parameters that affect the connection relationship: VMS and LMS.

2) ANALYSIS OF SATELLITE-GROUND LINK SWITCHING BASED ON VMS AND LMS

If we shield LMS and observe VMS, we see in Fig. 8 that satellite $S_{m,n-1}$ starts to move at time T_0 and arrives at the position of satellite $S_{m,n}$ at time T_1. The time required is defined as satellite time interval t_s, which can be derived from
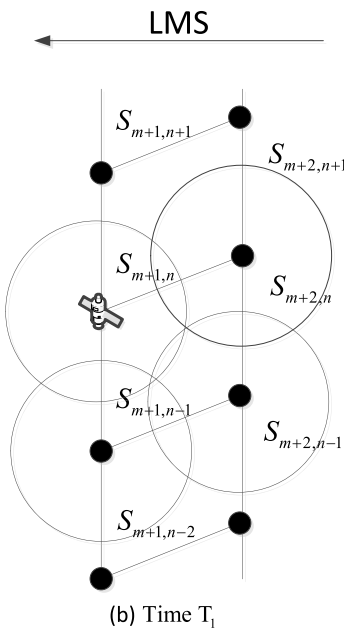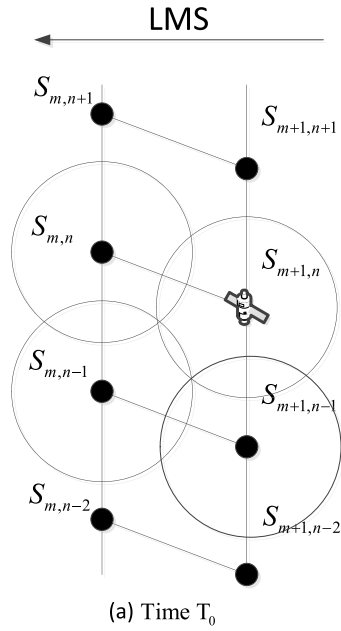
(a) Time T_0

FIGURE 10. **Switching time of connected satellites caused by VMS and LMS.**

formula (8).

$$t_E = T_1 - T_0 = \frac{2\pi}{N \cdot \omega_E} \qquad (8)$$

Considering the switching timing, as shown in Fig. 10, the interval between the track surface $m + 1$ and the track surface $m + 1$ is divided into two parts, namely, region A and region B. The coverage areas of satellite $S_{m+1,n}$ and satellite $S_{m+1,n-1}$ are divided into two parts, namely, region C and region D. B_{DN} is connected with $S_{m+1,n}$, which falls in region A in the direction of LMS and region C in the direction of VMS. According to the analysis in the previous section, in the next connected period, the satellite node connected to B_{DN} can only be one of the three nodes, namely, $S_{m+1,n-1}$, $S_{m+2,n}$, or $S_{m+2,n-1}$. Assume that the longitude and latitude coordinates of B_{DN} are (α, β) and those of the satellite node connected to B_{DN} are (α_s, β_s).

Define the time at which B_{DN} reaches the boundary between region A and region B as the longitude arrival time (LOAT) t_α, which can be derived from (9).

$$t_\alpha = \frac{\pi/2N + \alpha_S - \alpha}{\omega_E} \qquad (9)$$

Define the time when B_{DN} reaches the boundary between region C and region D as the latitude arrival time (LAAT) t_β, which can be derived from (10).

$$t_\beta = \frac{\pi/V + \beta_S - \beta}{\omega_S} \qquad (10)$$

Three kinds of connectivity between B_{DN} and the connected satellite can exist after switching: switching between adjacent nodes on the same orbital plane, switching between

(b) Time T_1

FIGURE 9. **Analysis of satellite motion under LMS by shielding VMS.**

formula (7).

$$t_s = T_1 - T_0 = \frac{2\pi}{V \cdot \omega} = \frac{2\pi}{V} \cdot \left[\frac{GM}{(R_{earth} + h)^3} \right]^{-0.5} \qquad (7)$$

Now, we shield VMS and observe LMS. As shown in Fig. 9, satellite $S_{m+1,n}$ starts to move at time T_0 and arrives at time T_1 at the position of the orbital surface where satellite $S_{m,n}$ was located at time T_0. The time required is defined as the orbital surface time interval t_E, which can be derived from
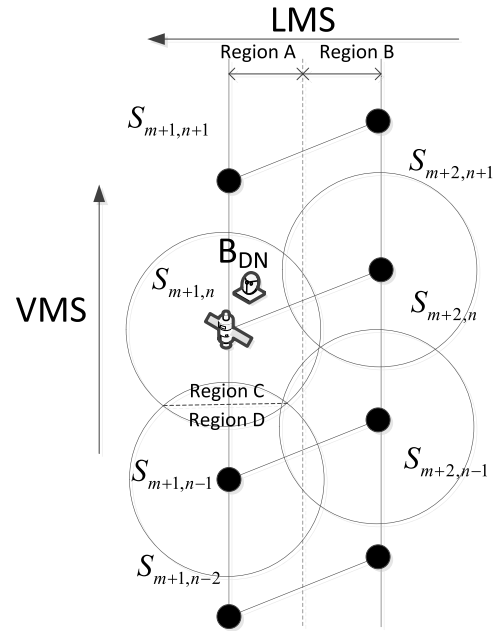
TABLE 2. The switching relationship between ground station and connected satellites.

Size relationship between t_α and t_β	Connected satellite selection	Satellite switching type
$t_\alpha > t_\beta$	$S_{m+1,n-1}$	switching between adjacent nodes on the same orbital plane
$t_\alpha = t_\beta$	$S_{m+2,n}$	switching between adjacent nodes on different orbital planes
$t_\alpha < t_\beta$	$S_{m+2,n-1}$	switching between nonadjacent nodes on different orbital planes

adjacent nodes on different orbital planes, and switching between nonadjacent nodes on different orbital planes. The switching relationship between B_{DN} and connected satellites is shown in Table 2.

IV. OPTIMIZATION STRATEGY

To solve the problem of SGLSI and ensure that the destination node can effectively receive data when the source node has a temporary transmission task, we consider optimizing the snapshot at the source node and aim for reliable data reception at the destination node. This paper proposes two strategies: the source preplanning calculation (SPPC) and the destination readdressing calculation (DRAC).

A. SOURCE PREPLANNING CALCULATION

The main reasons for the interruption of satellite-ground link switching are the randomness of data transmission and the switching between the ground station and connected satellites. Therefore, on the basis of the snapshot routing algorithm, the path from B_{SN} to B_{DN} and the required propagation time are known in advance, which enables the calculation of the exact time stamp of the destination node satellite under the path. Thus, a data routing strategy can be determined based on the connection of the corresponding satellite and the ground station under the time stamp by means of the following steps.

1. There comes a need to send data P, which can be determined by (11):

$$P = \sum_{i=1}^{k} p_i \qquad (11)$$

where p_i is a data packet, k is the total number of the data packets, i is the serial number of the packet, that is, P is divided into k pieces of data to be sent. B_{SN} determines the transmission time and records the transmission time stamp T_0.

2. B_{SN} determines the destination ground station B_{DN} and destination satellite node S_{DNm} connected to B_{DN} at this time. The connectivity maintaining period is t_m:

$$t_m = [T_{mB}, \quad T_{mE}] \qquad (12)$$

T_{mB} is the time when B_{DN} and S_{DNm} start to connect and T_{mE} is the time when the connection ends.

3. B_{SN} calculates the propagation delay t_{trans} and transmission delay t_{data} according to the given routing strategy π based on the data size of P, the transmission bandwidth, the satellite receiving and sending bandwidth and the buffer capacity.

4. The reception status of S_{DNm} is determined and, the data packet transmission in period t_m is considered. We assign m = 1 and obtain P_{trans}:

$$P_{trans} = \begin{cases} \sum_{i=1}^{k} p_i & (T_0 + t_{trans} + t_{Data}) \leq T_{1E} \\ \sum_{i=1}^{\left\lceil \frac{k(T_{1E}-T_0)}{t_{trans}+t_{Data}} \right\rceil} p_i & T_{1E} < (T_0 + t_{trans} + t_{Data}) \leq 2T_{1E} - T_{1B} \end{cases}$$

$$(13)$$

P_{trans} refers to the amount of data packets transmitted in B_{DN}. We can also obtain P_{keep}:

$$P_{keep} = \begin{cases} 0 & (T_0 + t_{trans} + t_{Data}) \leq T_{1E} \\ \sum_{i=\left\lceil \frac{k(T_{1E}-T_0)}{t_{trans}+t_{Data}} \right\rceil + 1}^{k} p_i & T_{1E} < (T_0 + t_{trans} + t_{Data}) \leq 2T_{1E} - T_{1B} \end{cases}$$

$$(14)$$

P_{keep} represents the amount of data packets that are reserved but not transmitted at S_{DN1}. Some large data packets cannot be transmitted in one communication period and need to be retransmitted in the subsequent communication period.

5. Step 4 is repeated until no data packets are reserved. The number of periods needed for the transmission of all the data packets is M, and M path plans are developed.

The advantage of adopting SPPC is that the transmission timing of data packets can be planned in advance, so data packets that cannot be transmitted in one communication period are reserved and continued in the next communication period, thereby ensuring the integrity of the data packets. This method is applicable for situations with few parallel tasks or small loads. However, when the network is congested due to high load in the network, unpredictable delays are likely to occur, causing the propagation time calculated by the ground station at the source node to be less accurate, thereby resulting in transmission failure based on the established strategy.

B. DESTINATION READDRESSING CALCULATION

In contrast to SPPC, in DRAC, the sending time of the source node can be ignored, and the analysis focuses on the destination node satellite and destination node ground station.

As shown in Fig. 11, B_{DN} is connected to S_{DN1} at time T_1 in connection period t_1. S_{DN1} has received data packet p_1 transmitted from relay node satellite S_{TN} and sends it to connection ground station B_{DN}. S_{TN} then sends the next data packet p_2 to S_{DN1}.

As shown in Fig. 12, B_{DN} is connected to S_{DN2} at time T_2 in connection period t_2, and data package p_1 has reached
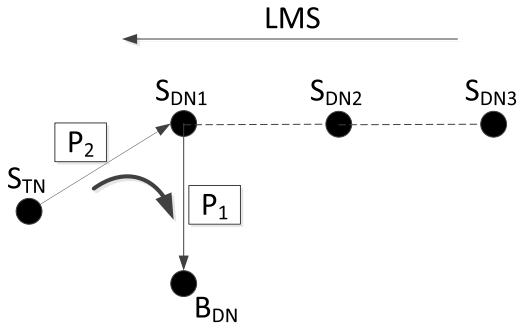
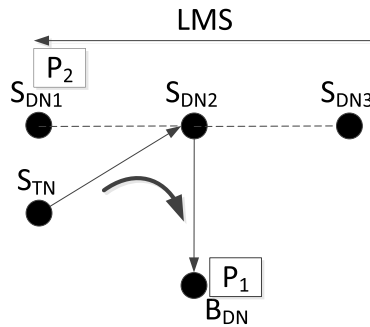**FIGURE 11.** Transmission path at time T$_1$ in connected period t$_1$.

FIGURE 12. Transmission path at time T$_2$ in connected period t$_2$.

B$_{DN}$ while data package p_2 has reached S$_{DN1}$. According to the originally planned routing strategy, the next destination address of data package p_2 sent by S$_{DN1}$ should be B$_{DN}$, but the link has been interrupted and the transmission cannot be completed. Under these circumstances, S$_{DN1}$ can transfer data to B$_{DN}$ by replacing the next hop destination node, which is the core idea of DRAC. The satellite must have some on-board processing capacity to conduct path replacement. Given the shortage of resources and limited load on LEO satellites, the computational complexity should be minimized.

1. Data packet p_i reaches the last satellite node S$_{DNk}$ in the planned path, and S$_{DNk}$ looks for the connected ground station. If B$_{DN}$ exists and the destination address is the same, S$_{DNk}$ will send data packet p_i to B$_{DN}$ to complete the transmission; if there is no ground station or the destination address is different, proceed to step 2.

2. Complete address searching. S$_{DNk}$ can roughly identify the current connection satellite of the destination node ground station at the current time. The calculation is as follows:

a. Record current time stamp T$_{now}$ and the latitude and longitude (α_s, β_s) of the S$_{DNk}$ at this time. Read the time stamp T$_0$ sent by the packet and calculate the longitude and latitude (α'_s, β'_s) of the node at time T$_0$.
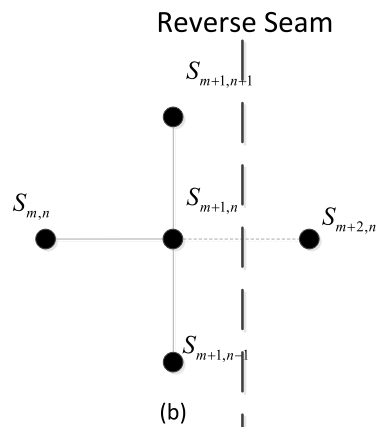
b. Calculate LOAT t'_α and LAAT t'_β at time T$_0$ and compare t'_α and t'_β. If $t'_\alpha \leq t'_\beta$, go to step c; if $t'_\alpha > t'_\beta$, go to step d.

c. The data packet is transmitted to a neighboring node on a different orbital plane in the opposite direction of LMS.

d. The data packet is transmitted to a neighboring node on the same orbital plane, and the transmission direction is the reverse direction of VMS.
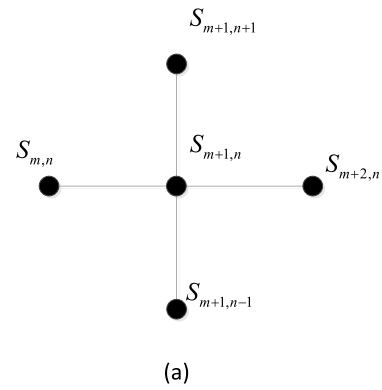
FIGURE 13. The connected node of a satellite consists of two neighbor satellites on the same orbital plane and two neighbor satellites on a different orbital plane.

3. S$_{DNk}$ sends packet p_i to S$_{DN(k+1)}$. If B$_{DN}$ exists, packet p_i is sent to B$_{DN}$ to complete transmission. If there is no connected ground station or the destination address is different, the packet is transmitted to a neighboring node in the same orbital plane, and the transmission direction is the reverse direction of VMS. The strategy ends.

This strategy consumes minimal satellite resources because the satellite must consider at most two hops of transmission. Next, we analyze whether two-hop transmission can complete the strategy.

As shown in Fig. 13, any satellite has at most 4 neighboring nodes. When the satellite is on both sides of the reverse seam, it has only 3 neighbors.

We first analyze a satellite with four neighboring nodes, taking $S_{m+1,n}$ as an example, as shown in Fig. 14. In the previous analysis, we see there is a possibility that the ground station switches to connect to $S_{m+2,n-1}$ after having connected with $S_{m+1,n}$, but since $S_{m+1,n}$ is not directly connected to $S_{m+2,n-1}$, $S_{m+2,n}$ is needed to complete the relay. Therefore, in the design process, if a data shift to the right occurs, the data are first transmitted to $S_{m+2,n}$. If $S_{m+2,n}$ is not covered by the node, the data are then directly transmitted to adjacent node $S_{m+2,n-1}$ on the same orbital surface.

(a)

(b)
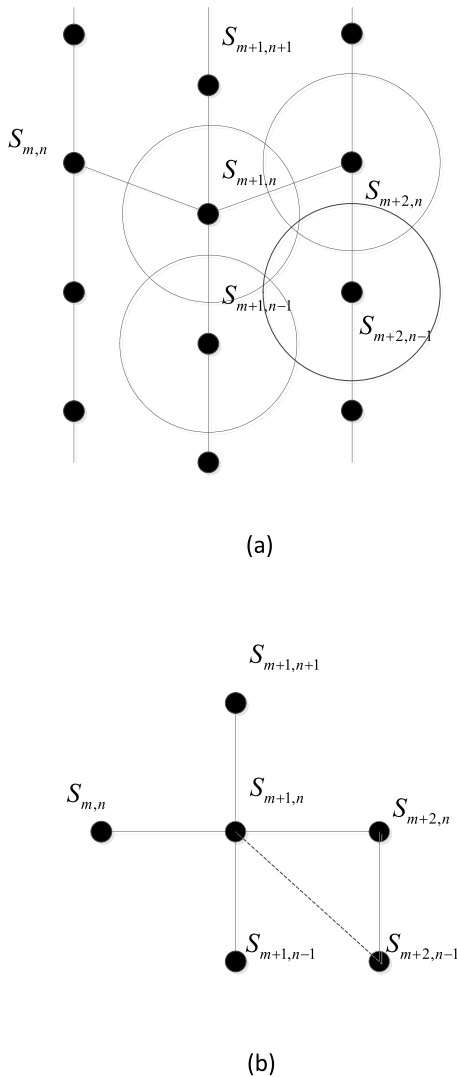
FIGURE 14. The connected node of a satellite consists of two neighbor satellites on the same orbital plane and two neighbor satellites on a different orbital plane.

We now consider whether there exist other nodes satisfying the conditions. Under the original routing plan, the default destination node satellite is $S_{m+1,n}$. Since SGLSI occurs when the destination node satellite and ground station switch, the destination node satellite will begin to switch shortly after the data packet is sent.

The connection period of the new destination satellite with the destination ground station is on the order of minutes, while the transmission time is on the order of milliseconds. Therefore, even in the case of extreme congestion, the transmission time will not exceed the second level. As a result, during the connection period of the new destination satellite, the data packet will definitely reach the destination. If the delay is greater than the minute level, it would be better to retransmit the data than to have the satellite look for the address again.

V. SIMULATION AND RESULTS

This paper proposes two strategies, namely, SPPC and DRAC, to solve the problem of SGLSI. By determining in advance the time when data packets arrive at the destination node and making alternative planning on the ground, SPPC ensures that the destination node satellite is able to transmit the data to the destination node ground station. By contrast, DRAC identifies the destination node ground station by updating the route according to the calculation by the destination mode satellite based on a snapshot.

To compare and analyze the performance of the network when SGLSI occurs, this paper constructs a global coverage constellation network based on polar orbit to build the network simulation model, with constellation parameters of $11 \times 10/10/5 : 600km : 90$. In this paper, Satellite Tool Kit (STK) and OPNET are used to simulate the LEO satellite constellation model. STK software is used to generate intersatellite links and the connection between satellites and ground stations. OPNET software is used to simulate the sending of data packets. Because OPNET is based on event-driven simulation, STK is needed simulate link connectivity.

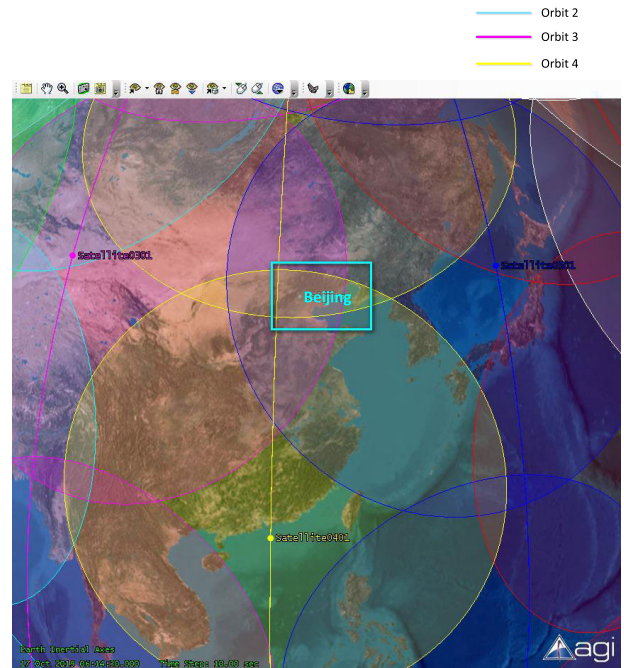### A. CONSTELLATION MODEL SIMULATION

By means of STK, we establish a global network of LEO polar satellites that has 10 orbital planes, each containing 11 satellites. The orbital height of the satellites is 600 kilometers. The network model has two ground stations, namely, Beijing and New York, that transfer simulation data. The simulation model is shown in Fig. 15. The New York and Beijing ground stations are located in the rectangular boxes, and data are transmitted from the former to the latter. As the source node ground station, New York is used only to calculate the route cost of data, it has little impact on the result of the simulation. Therefore, the destination node ground station Beijing, specifically the problem of satellite-ground link switching, will be the focus of our study. Below is the analysis of Beijing's satellite-ground link switching conducted via STK.

In STK, we simulate the connection between the satellite and ground station for a certain period of time. As shown in Fig. 16, the simulated starting time is 04:02:30 of October 17, 2019, and the ending time is 06:14:30 of October 17, 2019. The simulation duration is 120 minutes, and the time interval of each simulation is 10 seconds. The rectangular box indicates the position of the Beijing ground station. During this time period, the satellite shown in the figure is moving downward.
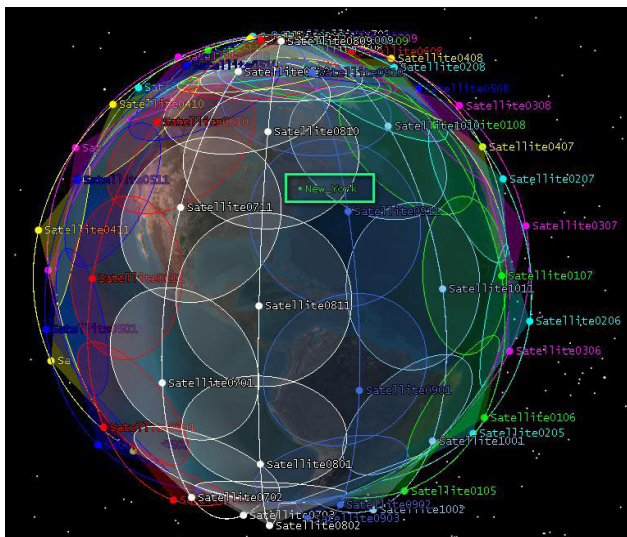
As shown in Fig. 17, from the simulation of the satellite-ground connecting relationship of the Beijing ground station, it can be seen that the switching of satellites connected with the ground station takes place over a period of time, and the switching time interval is basically the same. The link holding time of the simulation model is approximately 8 minutes and 50 seconds. After this period of switching on one
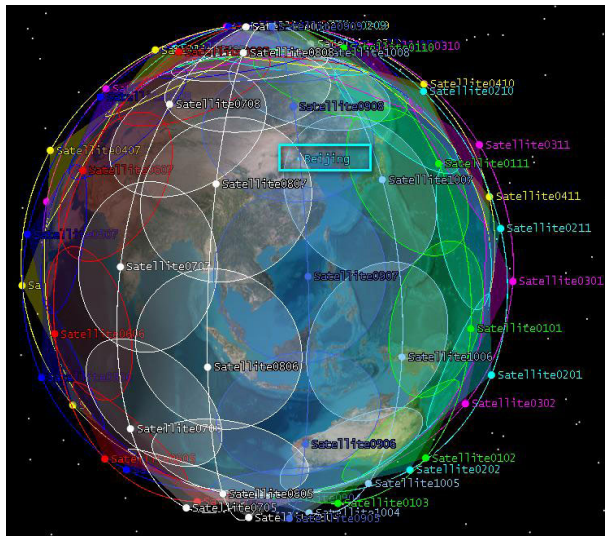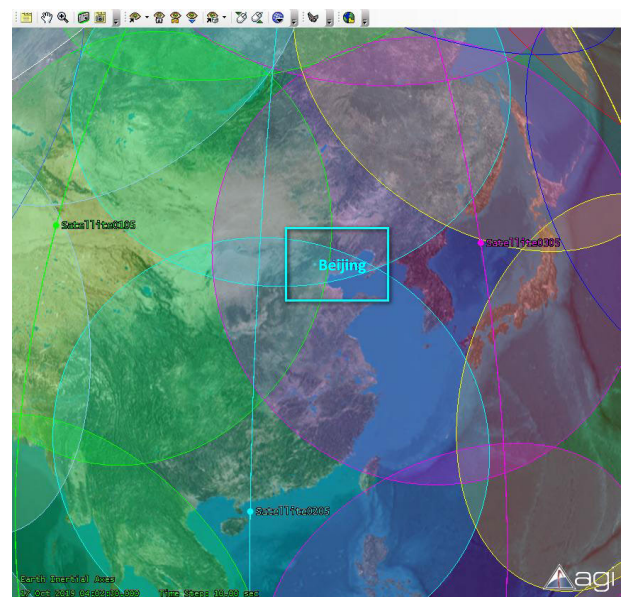
（a）Aerial view over Beijing

（b）Aerial view over New York

FIGURE 15. Model construction of the New York source node ground station and Beijing destination node ground station based on STK.

orbital surface, the switched satellite will move to its adjacent orbital surface. In the simulation, one of the two cross-orbital switches is the switching from satellite 203 to satellite 303, and the other is from satellite 306 to satellite 405. Satellite 203 is directly connected to satellite 303, so data can be transmitted directly. By contrast, satellite 306 and satellite 405 are not directly connected, so the data transmission path is satellite 306-406-405. Moreover, the transmission direction from satellite 406 to satellite 405 is the reverse direction of satellite movement (upward), which is consistent with the analysis in section III.

（a）Simulation start state

（b）Simulation end state

FIGURE 16. Satellite-ground link switching scenario based on STK.

B. SATELLITE-GROUND LINK TRANSMISSION MODEL SIMULATION

As shown in Fig. 18, we use OPNET to simulate packet loss before and after switching. In section II, we discussed when and how the problem of SGLSI occurs. Since SGLSI occurs only at the time of transmission between a destination node satellite and a destination node ground station, we simplify the source node and relay nodes in OPNET. According to the STK simulation results, 7 satellite nodes are needed to
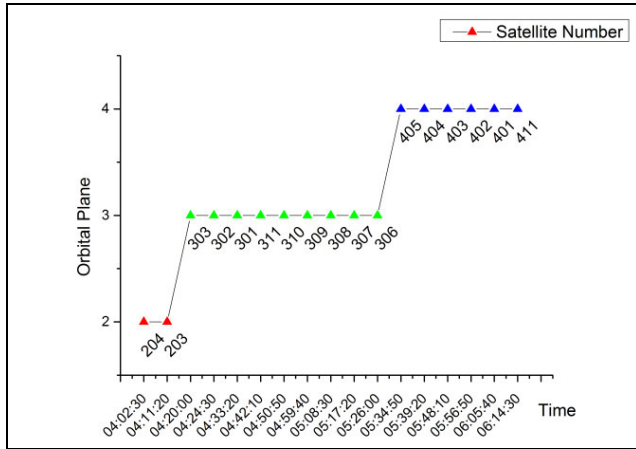
FIGURE 17. When the satellite-ground link is switched, the orbit will change and can be maintained in the same orbit.
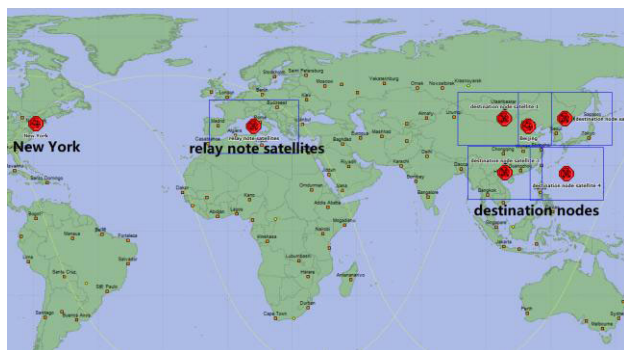

FIGURE 18. Simplified simulation diagram of source node and relay nodes in the network in OPNET.

FIGURE 19. Simulation analysis of three kinds of links before and after the satellite-ground link switching.

FIGURE 20. Comparison of the packet loss rates of three strategies with a random queuing delay of 0 ms.

relay a transmission from New York to Beijing. Because the space segment routing algorithm will not affect the simulation results of SGLSI, we can simulate the space segment routing transmission using Dijkstra's algorithm and focus exclusively on data transmission of the destination node satellite and destination node ground station.

Satellite switching can be classified into three situations, namely, switching between adjacent nodes on the same orbital plane, switching between adjacent nodes on different orbital planes and switching between nonadjacent nodes on different orbital planes. Therefore, our simulation must include all the above situations. As shown in Fig. 19, before satellite-ground link switching, the satellite connected to Beijing was destination node satellite1, and the satellites connected to Beijing after satellite-ground link switching are destination node satellite2, destination node satellite3 and destination node satellite4. The switching between Beijing and its satellite is simulated 100 times in all three situations, and the results are averaged. Furthermore, the ratio of unreceived data packets and data packets that should have been received in Beijing, that is, the packet loss rate, is calculated.

The simulation time is from 1 second before the switching moment to 2 seconds after switching, which is 3 seconds in total. The random packet loss rate of each hop in intersatellite transmission is 1%, and queuing delay is added to the simu-
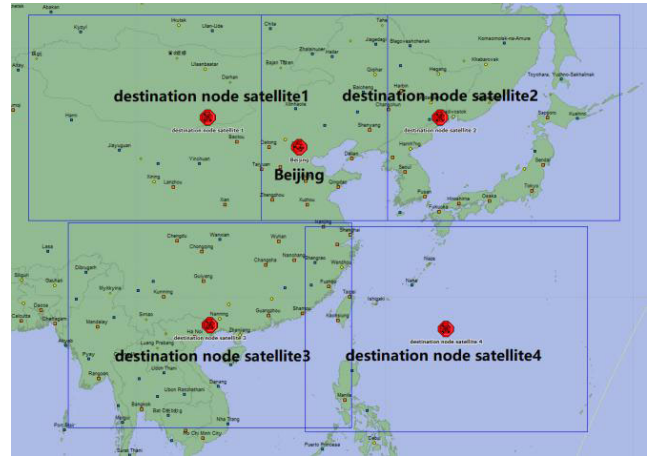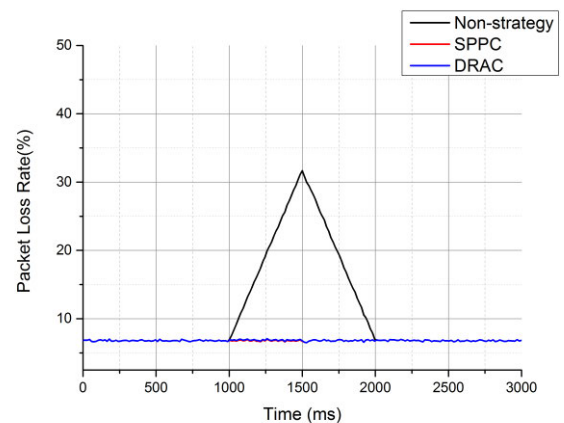
lation. The maximum transmission rate of a single satellite is 10 MBps, and the ground station's receive buffer is 20 MB.

In this paper, the focus is the problem of satellite handoff of satellites connected to the ground station. Therefore, the satellite routing transmission of the space segment can be simplified. According to [31], we set the transmission time of the space segment to 500 ms. Therefore, under the premise that the network has no queuing delay, the duration of the SGLSI is 500 ms. The three types of switching are simulated and analyzed under the strategies of SPPC and DRAC, as well as nonstrategy transmission. When the original destination satellite sends data, the percentage of discarded packets in the cache queue due to failure to find the correct next hop node is counted. In the simulation, the packet loss rate is considered both without and with queue delay of 100 ms and 300 ms.

The respective packet loss rates of Beijing under the three transmission strategies in the absence of random queuing delay are compared in Fig. 20.

When the network is not busy, if no strategy is adopted, large date packet loss is likely to occur after satellite-ground link switching due to the change in connected satellite. In this case, SPPC and DRAC can effectively avoid packet loss.
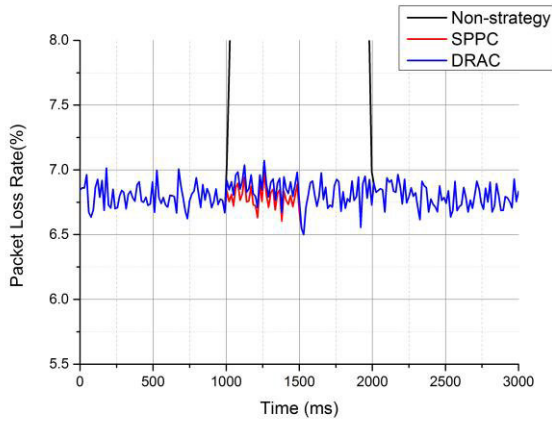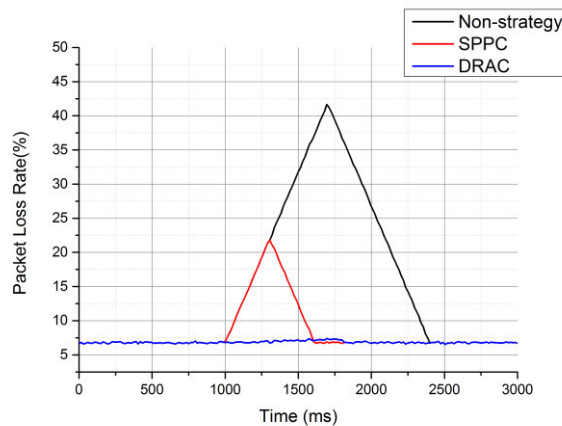
FIGURE 21. Comparison of the packet loss rates of SPPC and DRAC with a random queuing delay of 0 ms.
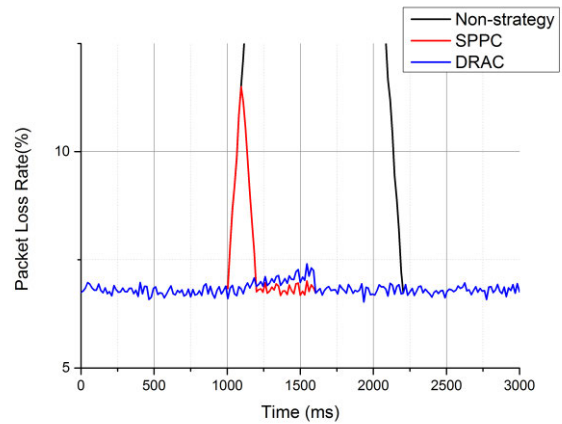
FIGURE 23. Comparison of the packet loss rates of SPPC and DRAC with a random queuing delay of 100 ms.
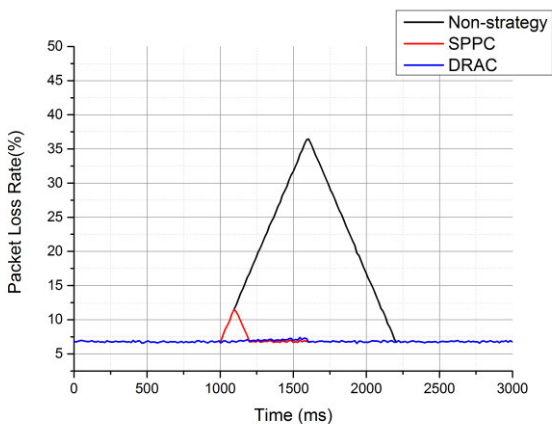
FIGURE 22. Comparison of the packet loss rates of the three strategies with a random queuing delay of 100 ms.

FIGURE 24. Comparison of the packet loss rates of the three strategies with a random queuing delay of 300 ms.

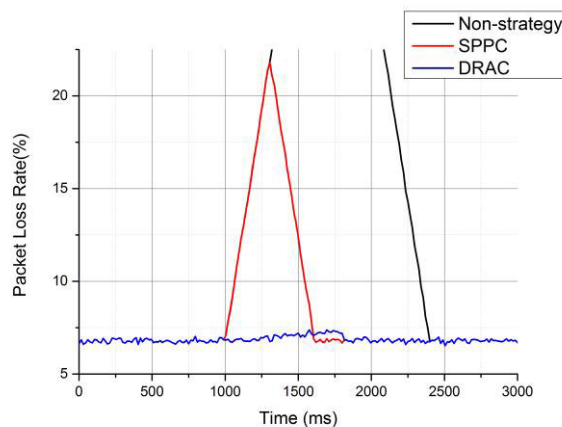**FIGURE 25.** Comparison of the packet loss rates of SPPC and DRAC with a random queuing delay of 300 ms.

As shown in Fig. 21, the packet loss rate of SPPC is slightly lower than that of DRAC because the transmission of DRAC increases the number of hops in the network, thereby slightly increasing the packet loss rate. Therefore, the packet loss rate of SPPC is even smaller without network queuing delay.

The packet loss rates of Beijing under three transmission strategies when the random queuing delay is 100 ms are compared in Fig. 22.

Because of the 100 ms queuing delay in the network, a large continuous packet loss occurs after satellite-ground link switching due to the change in connected satellite. When SGLSI occurs, the packet loss rate of SPPC increases first and then decreases, whereas the packet loss rate of DRAC remains stable within a small range.

As shown in Fig. 23, although the packet loss rate of SPPC can be lower than that of DRAC for a period of time after SGLSI, when SGLSI occurs, the packet loss rate of SPPC is much higher than that of DRAC. Since SPPC cannot predict the queuing delay caused by congestion in the network, unacceptable packet loss will occur. Only DRAC can effectively avoid packet loss in this scenario.

The packet loss rates of Beijing under the three transmission strategies when the random queuing delay is 300 ms are compared in Fig. 24.

When the queuing delay of the network is 300 ms, if no strategy is adopted after satellite-ground link switching, packet loss will continue to increase. The number of packets lost is close to half of the total number of packets. At this time, the received data are no longer available.
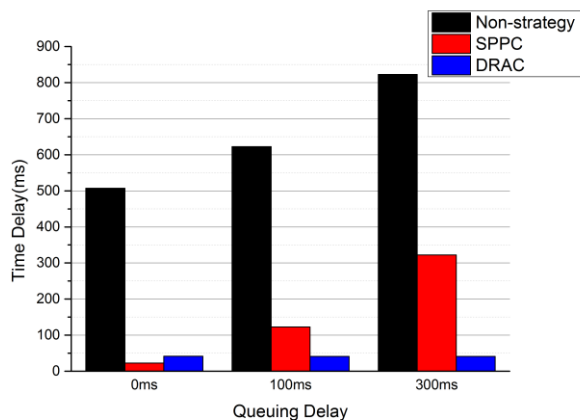
FIGURE 26. Comparison of the time delay of the three strategies.

As shown in Fig. 25, when SGLSI occurs, SPPC's packet loss time continues to increase for a period of time and then decreases, whereas DRAC's packet loss rate remains stable within a small range. Without being able to predict the queuing delay, SPPC can only partially prevent packet loss. Only DRAC can effectively avoid packet loss when there is queuing delay.

In addition to the packet loss rate, the data arrival time at the ground station of the destination node is an important research index. In the simulation, the time delay from the original destination satellite to the destination ground station is determined when SGLSI occurs, and the effect of the queuing time delay on the three strategies is studied. The corresponding time of a single satellite should not exceed 20 ms, including intersatellite transmission delay. The transmission time from the satellite to the earth station is determined by only the distance from the earth, and the orbit height is 600 km.

As shown in Fig. 26, regardless of whether there is queuing delay, if no strategy is adopted, a large time delay is observed. SPPC has the minimum time delay when the load is small and there is no queuing delay. However, as the queuing delay increases, the time delay of SPPC also increases. Therefore, when the network load is large, DRAC can ensure a small time delay.

VI. CONCLUSION

By analyzing the packet loss rate of zenith-passing satellites under different queuing delays, we find that SPPC and DRAC both effectively avoid packet loss in the absence of queuing delay. In addition, the effect of SPPC is better than that of DRAC because SPPC can predict which satellite will eventually be connected to the ground station, whereas DRAC must pass through one or two more satellites to find it. When queuing delay due to unpredictable factors exists in the network, SPPC cannot prevent all packet loss because SPPC updates the routing timetable in advance by estimating the data transmission delay and propagation delay in the network. Although this strategy does not consume much of the computing resources of the satellite, it is difficult to effectively

identify the situation in the network. DRAC, by contrast, is a dynamic routing strategy that can effectively avoid the packet loss caused by queuing delay. Moreover, DRAC consumes even less computing resources because it needs only to readdress the destination node satellites.

In summary, SPPC and DRAC can both avoid the problem of SGLSI to some extent. However, SPPC requires that the network transmission in the space segment not be congested because SPPC cannot effectively address the handover interruption caused by unpredictable delay. In contrast, DRAC can effectively address unpredictable network congestion, but it needs to go through one or two more satellites to find the satellite that will eventually be connected to the ground station, which results in some packet loss. In addition, DRAC must use some of the processing capacity of the satellite to identify the satellite that will be connected to the ground station in the next period of time, which is more demanding for the design of the satellite.

This paper focuses on the route of the "last hop" of the satellite-ground link. The selected ground station is relatively fixed by ignoring the space segment. In subsequent research, we will integrate SPPC and DRAC and combine existing spatial segment routing strategies to verify the performance of the network with respect to the whole path. Moreover, we will consider the routing link switching of ground equipment in high-speed mobile applications.

REFERENCES

[1] J.-C. Jeong, M. Uhm, D.-P. Jang, and I.-B. Yom, "A Ka-band GaAs multi-function chip with wide-band 6-bit phase shifters and attenuators for satellite applications," in *Proc. 13th Eur. Conf. Antennas Propag. (EuCAP)*, Krakow, Poland, Mar./Apr. 2019, pp. 1–4.
[2] T. Debogovic, P. Robustillo-Bayon, N. Saponjic, F. Bongard, M. Sabbadini, F. Tiezzi, and J. R. Mosig, "Low-profile multi-function antenna system for small satellites," in *Proc. 10th Eur. Conf. Antennas Propag. (EuCAP)*, Apr. 2016, pp. 1–5.
[3] M. Werner, "A dynamic routing concept for ATM-based satellite personal communication networks," *IEEE J. Sel. Areas Commun.*, vol. 15, no. 8, pp. 1636–1648, Oct. 1997.
[4] M. Werner, G. Berndl, and B. Edmaier, "Performance of optimized routing in LEO intersatellite link networks," in *Proc. IEEE 47th Veh. Technol. Conf. Technol. Motion*, vol. 1, Nov. 2002, pp. 246–250.
[5] T. H. Chan, B. S. Yeo, and L. F. Turner, "A localized routing scheme for LEO satellite networks," in *Proc. AIAA 21st Int. Commun. Satell. Syst. Conf. Exhibit (ICSSC)*, Yokohama, Japan, 2003, pp. 2357–2364.
[6] I. F. Akyildiz, E. Ekici, and M. D. Bender, "MLSR: A novel routing algorithm for multilayered satellite IP networks," *IEEE/ACM Trans. Netw.*, vol. 10, no. 3, pp. 411–424, Jun. 2002.
[7] E. Ekici, I. F. Akyildiz, and M. D. Bender, "A distributed routing algorithm for datagram traffic in LEO satellite networks," *IEEE/ACM Trans. Netw.*, vol. 9, no. 2, pp. 137–147, Apr. 2001.
[8] K. Tsai and R. P. Ma, "DARTING: A cost-effective routing alternative for large space-based dynamic-topology networks," in *Proc. MILCOM*, vol. 2, Nov. 2002, pp. 682–686.
[9] R. A. Raines, R. F. Janoso, D. M. Gallagher, and D. L. Coulliette, "Simulation of two routing protocols operating in a low Earth orbit satellite network environment," in *Proc. MILCOM*, vol. 1, Nov. 2002, pp. 429–433.
[10] J.-H. Song, V. Wong, and V. C. M. Leung, "Load-aware on-demand routing (LAOR) protocol for mobile ad hoc networks," in *Proc. 57th IEEE Semiannu. Veh. Technol. Conf. (VTC-Spring)*, vol. 3, Apr. 2004, pp. 1753–1757.
[11] W. Zhaofeng, H. Guyu, Y. Seyedi, and J. Fenglin, "A simple real-time handover management in the mobile satellite communication networks," in *Proc. 17th Asia-Pacific Netw. Oper. Manage. Symp. (APNOMS)*, Aug. 2015, pp. 175–179.

[12] B. Yang, Y. Wu, X. Chu, and G. Song, "Seamless handover in software-defined satellite networking," *IEEE Commun. Lett.*, vol. 20, no. 9, pp. 1768–1771, Sep. 2016.

[13] M. Gkizeli, R. Tafazolli, and B. Evans, "Modeling handover in mobile satellite diversity based systems," in *Proc. IEEE 54th Veh. Technol. Conf. (VTC Fall)*, vol. 1, Nov. 2002, pp. 131–135.

[14] M. Gkizeli, R. Tafazolli, and B. G. Evans, "Hybrid channel adaptive handover scheme for non-GEO satellite diversity based systems," *IEEE Commun. Lett.*, vol. 5, no. 7, pp. 284–286, Jul. 2001.

[15] Y. Seyedi and S. M. Safavi, "On the analysis of random coverage time in mobile LEO satellite communications," *IEEE Commun. Lett.*, vol. 16, no. 5, pp. 612–615, May 2012.

[16] X. Hu, H. Song, S. Liu, and W. Wang, "Velocity-aware handover prediction in LEO satellite communication networks," *Int. J. Satell. Commun. Netw.*, vol. 36, no. 6, pp. 451–459, Nov. 2018.

[17] Z. Wu, F. Jin, J. Luo, Y. Fu, J. Shan, and G. Hu, "A graph-based satellite handover framework for LEO satellite communication networks," *IEEE Commun. Lett.*, vol. 20, no. 8, pp. 1547–1550, Aug. 2016.

[18] C. Fuchs and F. Moll, "Ground station network optimization for space-to-ground optical communication links," *J. Opt. Commun. Netw.*, vol. 7, no. 12, p. 1148, Dec. 2015.

[19] S. Cakaj, B. Kamo, A. Lala, and A. Rakipi, "Elevation impact on signal to spectral noise density ratio for Low Earth Orbiting satellite ground station at S-band," in *Proc. Sci. Inf. Conf.*, Aug. 2014, pp. 641–645.

[20] M. Fischer and A. L. Scholtz, "Design of a multi-mission satellite ground station for education and research," in *Proc. 2nd Int. Conf. Adv. Satell. Space Commun.*, Jun. 2010, pp. 58–63.

[21] C. Partridge and T. J. Shepard, "TCP/IP performance over satellite links," *IEEE Netw.*, vol. 11, no. 5, pp. 44–49, Sep./Oct. 1997.

[22] Y. Sik Kim, Y.-H. Bae, Y. Kim, and C. Hye Park, "Traffic load balancing in low Earth orbit satellite networks," in *Proc. 7th Int. Conf. Comput. Commun. Netw.*, Nov. 2002, pp. 191–195.

[23] Z. Tang, Z. Feng, B. Zhao, and C. Wu, "Link reassignment based snapshot partition for polar-orbit LEO satellite networks," 2014, p. 6, *arXiv:1411.0372*. [Online]. Available: https://arxiv.org/abs/1411.0372

[24] Z. Tang, C. Wu, Z. Feng, W. Yu, B. Zhao, and W. Han, "Rollback links characterization for the snapshot routing algorithm in polar-orbit satellite networks," *IEICE Trans. Commun.*, vol. E98.B, no. 8, pp. 1715–1724, 2015.

[25] P. Francois and O. Bonaventure, "Avoiding transient loops during the convergence of link-state routing protocols," *IEEE/ACM Trans. Netw.*, vol. 15, no. 6, pp. 1280–1292, Dec. 2007.

[26] H. Peterson, S. Sen, J. Chandrashekar, L. Gao, R. Guerin, and Z.-L. Zhang, "Message-efficient dissemination for loop-free centralized routing," *SIGCOMM Comput. Commun. Rev.*, vol. 38, no. 3, p. 63, Jul. 2008.

[27] M. Bergmann, W. Gappmair, and O. Koudelka, "Parameter estimation for link adaptation on land-mobile satellite links," in *Proc. 9th Int. Symp. Commun. Syst., Netw. Digit. Sign (CSNDSP)*, Jul. 2014, pp. 1139–1143.

[28] Z. Hou, X. Yi, Y. Zhang, Y. Kuang, and Y. Zhao, "Satellite-ground link planning for leo satellite navigation augmentation networks," *IEEE Access*, vol. 7, pp. 98715–98724, 2019.

[29] W. Qin, P. Wei, and X. Yang, "The method on determining invisible satellite-ground clock difference with inter-satellite-link," in *Proc. IEEE Int. Freq. Control Symp. (IFCS)*, May 2016, pp. 1–5.

[30] Z. Xiaofang, H. Wang, W. Xiangjun, W. Jie, and C. Zhonggui, "GNSS coverage performance for medium-high earth orbital satellites," in *Proc. 26th Chin. Control Decis. Conf. (CCDC)*, May 2014, pp. 1902–1906.

[31] H. Yan, Q. Zhang, and Y. Sun, "A novel routing scheme for LEO satellite networks based on link state routing," in *Proc. IEEE 17th Int. Conf. Comput. Sci. Eng.*, Dec. 2014, pp. 876–880.

[32] S. Panko and M. Tsimbal, "The method of determining the speed of a spacecraft in a Low Earth Orbit personal satellite communication systems," in *Proc. Int. Siberian Conf. Control Commun. (SIBCON)*, Jun. 2017, pp. 1–3.

[33] N. Hamamoto, Y. Arimoto, Y. Hashimoto, T. Ide, and M. Sakasai, "High speed and global store and forward communication system using LEO satellites," in *Proc. 3rd IEEE Int. Conf. Universal Pers. Commun.*, Dec. 2002, pp. 418–422.

[34] Y. Wu, G. Hu, F. Jin, and J. Zu, "A satellite handover strategy based on the potential game in LEO satellite networks," *IEEE Access*, vol. 7, pp. 133641–133652, 2019.

[35] Z. Yi, L. Jun, S. Qian, J. Yong, and H. Yanlang, "Topology control strategy of LEO satellite constellation based on optimal polar boundary," in *Proc. Int. Conf. Electron., Commun. Control (ICECC)*, Sep. 2011, pp. 4605–4608.

[36] G. Yang, Y. Liu, M. Jin, and H. Liu, "A robust and adaptive control method for flexible-joint manipulator capturing a tumbling satellite," *IEEE Access*, vol. 7, pp. 159971–159985, 2019.

[37] A. Modiri, L. Mohammady, and N. Molanian, "Less faulty and simpler statistical prediction of sun-synchronous polar LEO satellite visions for ground stations," in *Proc. 4th Adv. Int. Conf. Telecommun.*, Jun. 2008, pp. 386–391.

[38] M. Kasal, "Remote controlled satellite ground station," in *Proc. 2nd Int. Conf. Recent Adv. Space Technol.*, Oct. 2006, pp. 442–444.

[39] P. Rezaei and M. Hakkak, "Evaluation of interaction effect between LEO ground station antennas," in *Proc. 18th Int. Conf. Appl. Electromagn. Commun.*, 2005, pp. 1–4.

[40] S. Humayun and M. H. Soomro, "Development of a test bed for monitoring & control software of a ground station & its analysis by application of standard software metrics," in *Proc. Int. Conf. Aerosp. Sci. Eng. (ICASE)*, Islamabad, Pakistan, Aug. 2013, pp. 1–5.

[41] S. Cakaj, W. Keim, and K. Malaric, "Intermodulation by uplink signal at low earth orbiting satellite ground station," in *Proc. 18th Int. Conf. Appl. Electromagn. Commun.*, Oct. 2005, pp. 1–4.

JIRUI ZHANG received the B.S. degree in information and communication engineering from Beijing Jiaotong University, China, in 2013, and the M.S. degree in information and communication engineering from the National University of Defense Technology, China, in 2015. He is currently pursuing the Ph.D. degree in communication and system with Space Engineering University. He has been jointly trained by the Beijing Institute of Tracking and Telecommunications Technology.

SHIBING ZHU was born in Hunan, China, in 1969. He received the B.S. degree from the Equipment College, China, in 1992, and the M.S. degree from National Defense University, China, in 1997, and the Ph.D. degree from the Wuhan University of Technology, China, in 2009. He is currently a Professor and a Doctoral Supervisor with Space Engineering University. His current research interests include spatial information network and security and 5G mobile communication.

HEFENG BAI was born in Yunnan, China, in 1971. He received the B.S., M.S., and Ph.D. degrees from the National University of Defense Technology. He is currently a Researcher with the Beijing Institute of Tracking and Telecommunications Technology, focusing on space-based information networks, space networks and routing, and space link transmission.

CHANGQING LI was born in Sichuan, China, in 1972. He received the B.S. and M.S. degrees from the Harbin Institute of Technology (HIT), China, in 1992 and 1998, respectively, and the Ph.D. degree from the Beijing University of Posts and Telecommunications (BUPT), China, in 2006. He is currently an Associate Professor and a Master Tutor with Space Engineering University. His current research interests include information science, wireless communication, and space networks.

● ● ●